

Distributed coherent manipulation of qutrits by virtual excitation processes

Zhen-Biao Yang,¹ Sai-Yun Ye,^{1,2} Alessio Serafini,² Shi-Biao Zheng^{1,*}

¹Department of Physics and State Key Laboratory Breeding Base of Photocatalysis, Fuzhou University, Fuzhou 350002, P. R. China

²Department of Physics & Astronomy, University College London, Gower Street, London WC1E 6BT, United Kingdom

*Corresponding author: sbzheng@pub5.fz.fj.cn

Abstract. We propose a scheme for the deterministic coherent manipulation of two atomic qutrits, trapped in separate cavities coupled through a short optical fibre or optical resonator. We study such a system in the regime of dispersive atom-field interactions, where the dynamics of atoms, cavities and fibre operates through virtual population of both the atomic excited states and photonic states in the cavities and fibre. We show that the resulting effective dynamics allows for the creation of robust qutrit entanglement, and thoroughly investigate the influence of imperfections and dissipation, due to atomic spontaneous emission and photon leakage, on the entanglement of the two qutrits state.

PACS numbers: 03.67.Mn, 42.50.Pq, 42.81.Qb

1. Introduction.

One of the crucial ingredients in the upcoming area of quantum technologies will be the capability of coherently manipulating quantum systems at a distance, such that *entanglement* (*i.e.*, quantum correlations) can be created between different nodes of a global quantum system.

Entanglement is one of the most peculiar features of quantum mechanics, and the most distinct signature of quantum coherence. Entangled states of two or more particles not only play an important role for tests of quantum nonlocality [1-3], but also lie at the heart of quantum information processing and quantum computing [4]. Entangled quantum states come in many flavours, such as Bell, Einstein-Podolsky-Rosen [1], Greenberger-Horne-Zeilinger [3], or W states [5], generally depending on the dimensionality and tensor product structure of the Hilbert spaces involved. All these states have different qualities and are suitable for different roles in quantum information protocols [3,5]. In this context, entangled states of multiple systems with Hilbert spaces of dimension d (*i.e.* of ‘qudits’, with $d > 2$) offer their specific advantages over the – archetypical and most commonly considered – entangled states of two-dimensional systems (of ‘qubits’). For instance, entangled states of two qudits violate local realism more strongly than entangled states of two qubits, and their entanglement is more resilient to noise [6]. Also, quantum cryptographic protocols where qubits are replaced with qudits are both more secure and faster (in that more information may be sent, on average, per sent particle) [7].

Entangled states can currently be generated in a variety of physical systems, such as trapped ions [8], quantum electrodynamics cavities (QED) [9], superconducting circuits [10], semiconductor quantum dots [11], linear optical systems [12] and impurity spins in solids [14]. Cavity QED [14], which concerns the interaction of atoms and photons inside optical cavities, provides experimentalists with a very favorable setting for the generation of entanglement. Atomic systems are qualified to act as qubits or, more generally, qudits, as appropriate internal electronic states can coherently store information over relatively long time scales. At the same time, in such systems photons are suitable for the transfer of information between distant nodes. High-finesse cavities can provide good insulation against the environment and can thus have long coherence times [15]. Two-atom Bell states, and three-particle (two atoms plus one photon) GHZ entangled states have been experimentally demonstrated with Rydberg atoms passing through a superconducting microwave cavity [16,17].

Schemes for the generation of entangled states of two ‘qutrits’ (*i.e.*, of two three level quantum systems) for two atoms via a single nonresonant cavity have also been proposed [18]. However, in order to be used for quantum communication protocols [19], such an entanglement should be generated between *distant* atoms, like atoms trapped in different cavities. “Distributed” atomic entanglement requires a way to coherently mediate the interaction between the two atoms. One way to establish this interaction is through coincidence detection of photons leaking out of the cavities [20]: in this way, entangled states are only probabilistically generated and the success probability is dependent on the efficiency of photon detectors. The other possibility is to directly link the cavities with an optical fibre, waveguide or by a third mediating cavity: entangled states can be deterministically generated in such a way [21,22]. Both types of quantum connectivity essentially allow for the distribution of entanglement across a quantum network [23].

In this paper, we shall present a way, based on the proper choice of atomic levels’

structure and operating regimes, to engineer a deterministic coherent interaction between two qutrits embodied by atoms trapped in distant cavities, linked by a third optical resonator. We will then move on to study the entanglement that can be generated by such an interaction, as well as its resilience to imperfections and quantum noise.

Before proceeding, let us first review some previous schemes for the deterministic generation of entangled states via such a type of connected cavities [22]. Several schemes have been proposed for the deterministic generation of several diverse kinds of entangled states [24–28], including Bell states [24], W states [28], GHZ states [26, 28], and also qutrit entangled states [25, 27]. In the schemes of Refs. [25, 26], the adiabatic passage along dark states is employed. These schemes [25, 26] are based on accurately tailored sequences of pulses and thus require a considerable degree of control. In other schemes [22, 24], the Rabi oscillations of the whole system composed of the atoms, cavity modes, and fibre modes is utilized; the entangled states are generated through the exchange of excitation numbers for the atoms and photons. Hence, such schemes [22, 24] are bound to be rather sensitive to atomic spontaneous emission and photon losses. In other schemes [27, 28], the population of the atomic excited states can be effectively suppressed by virtue of dispersive atom-field interactions, but the photonic states in the cavities or fibre are still populated, so that the whole system is still sensitive to photon losses.

The scheme we propose here is different from all such previous schemes [22, 24–28], even from those adopting adiabatic passage [25, 26]. The scheme is inspired by a previous idea for virtual-photon-induced phase gates between two distant atoms [29]. In the scheme, the entanglement is generated through virtual population of not only the atomic excited states but also the photonic states in the cavities and fibre. Therefore, our scheme will turn out to be well shielded from both atomic spontaneous emission and photon losses.

The paper is organized as follows. In Sec. 2, we specify our conditions on the physical parameters and derive the effective Hamiltonian for the system. In Sec. 3, we discuss the generation of two qutrit entangled state via the effective Hamiltonian and study the reliability of the entangled state in the presence of mismatches in the system’s parameters. In Sec. 4, we discuss the influence of atomic spontaneous emission and photon leakage on the entangled state. Sec. 5 contains some concluding remarks.

2. The model

The schematic of our setup is shown in Fig. 1. Two distant atoms are individually trapped in two double-mode cavities (A and B), which are connected by a third optical resonator, as shown in Fig. 1 (a). The linking resonator can be either a third cavity coupling the two distant cavities (like in a photonic crystal), or a ‘short’ (in a sense which will be specified shortly) optical fibre. For simplicity, we will henceforth refer to the linking resonator as to the “fibre”.

The coupling of the fibre modes to the modes of the cavities in Schrödinger interaction picture may be modeled by the Hamiltonian $H_I^{cf} = \sum_{n=1}^{\infty} \sum_{k=L,R} \Delta_{n,k} b_{n,k}^{\dagger} b_{n,k} + \nu_{n,k} \{b_{n,k} [a_{A,k}^{\dagger} + (-1)^n e^{i\varphi_f} a_{B,k}^{\dagger}] + H.c.\}$ ($\hbar = 1$ is used throughout this paper), where $\Delta_{n,k}$ is the frequency difference of the n th polarised fibre mode and the cavity mode with the corresponding polarisation (L and R denote, respectively, σ^{\dagger} -circular and

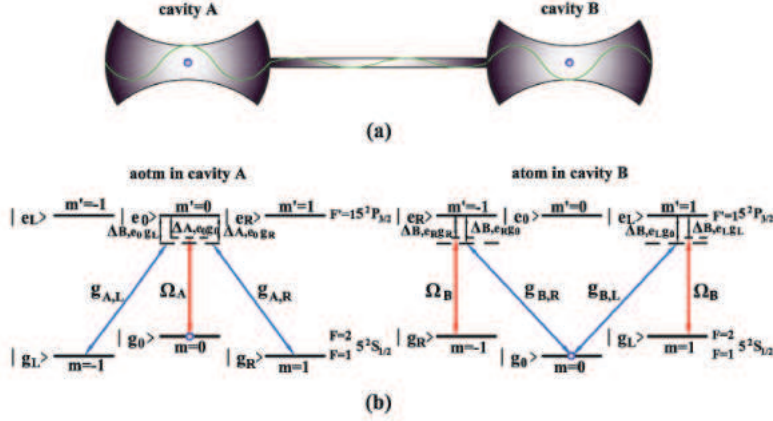


Figure 1. Setup and atoms' levels' configuration for realising qutrit entanglement. (a) Two atoms are trapped in the double-mode cavities A and B, respectively; the cavities are coupled by an optical fibre. (b) Possible implementation with ^{87}Rb atoms, showing the involved atomic transitions for each atom.

σ^- -circular polarisation), $b_{n,k}$ and $a_{A,k}$ ($a_{B,k}$) are the annihilation operators for the polarised modes of the fibre and of cavity A (B), $\nu_{n,k}$ is the corresponding coupling strength, and the phase φ_f is due to the propagation of the field through the fibre of length L : $\varphi = 2\pi\omega L/c$ [22]. In the short fibre limit $2L\bar{\nu}/(2\pi c) \ll 1$ [22], where $\bar{\nu}$ is the decay rate of the cavity fields into a continuum of the fibre modes, only the resonant modes b_L and b_R of the fibre are excited and coupled to the cavity modes. In this case, the interaction Hamiltonian H_I^{cf} describing the cavity-fibre coupling can be rewritten as [22,27]

$$H_I^{cf} = \sum_{k=L,R} \nu_k [b_k(a_{A,k}^\dagger + e^{i\varphi_f} a_{B,k}^\dagger) + H.c.]. \quad (1)$$

In this paper, the state of the photon modes for cavity A (B) or the fibre is taken to be $|ii'\rangle_s$ ($s = c_1, c_2$, and *fib*), with i (i') denoting i σ^\dagger - (i' σ^- -) photons.

The atoms have three excited states ($|e_L\rangle$, $|e_0\rangle$, and $|e_R\rangle$) and three ground states ($|g_L\rangle$, $|g_0\rangle$, and $|g_R\rangle$), which could be the Zeeman sublevels of alkali atoms in the excited- and ground-state manifold, respectively. To fix ideas and portraiture a case of practical interest, we consider here a possible implementation with ^{87}Rb , whose relevant atomic levels are shown in Fig. 1. (b). We only illustrate the involved state transitions by starting from the initial state $|g_0\rangle_A |g_0\rangle_B$ for the atoms. Each atom is assumed to be coupled (off-resonantly) to an external π -polarised classical field and both σ^\dagger - and σ^- -polarised photon modes of the local cavity.

We first describe the involved transitions for each atom in its local cavity. In cavity A, the transitions $|g_0\rangle \rightarrow |e_0\rangle$ and $|e_0\rangle \rightarrow |g_L\rangle$ ($|g_R\rangle$) are coupled to the π -polarised

classical field and the σ^\dagger -circular (σ^- -circular) polarised cavity mode, respectively. In cavity B, the transitions $|g_0\rangle \rightarrow |e_L\rangle$ ($|e_R\rangle$) and $|e_k\rangle \rightarrow |g_k\rangle$ are coupled to the σ^\dagger -circular (σ^- -circular) polarised cavity mode and the π -polarised classical field, respectively. It should be noted that, for the selected frequencies of the classical and cavity fields, additional transitions cannot be induced due to the large difference of the energy levels between the $F = 1$ and $F = 2$ states of the ground manifold $5^2S_{1/2}$. In interaction picture, the Hamiltonian describing the interaction of the atoms with the cavity and classical fields can then be written as

$$H_I^{acl} = \sum_{k=L,R} [g_{A,k} a_{A,k} e^{i\Delta_{A,e_0 g_k} t} |e_0\rangle_A \langle g_k| + \Omega_A e^{i\Delta_{A,e_0 g_0} t} e^{i\phi_A} |e_0\rangle_A \langle g_0| + g_{B,k} a_{B,k} e^{i\Delta_{B,e_k g_0} t} |e_k\rangle_B \langle g_0| + \Omega_B e^{i\Delta_{B,e_k g_k} t} e^{i\phi_B} |e_k\rangle_B \langle g_k| + H.c], \quad (2)$$

where $\Delta_{x,yz}$ ($x = A, B$; $y = e_0, e_L, e_R$; $z = g_0, g_L, g_R$) denotes the energy difference between the fields and the corresponding atomic transition $|y\rangle \leftrightarrow |z\rangle$ in cavity x ; $g_{x,k}$ is the coupling strength of the atom with the polarised photon mode in cavity x and satisfies $g_{x,k} = g_0 C_{m,m'}$ (with g_0 and $C_{m,m'}$ being the atom-cavity coupling constant and Clebsch-Cordan coefficient, respectively); Ω_x and ϕ_x are one-half Rabi frequency and phase of the classical field, and $H.c$ denotes Hermitian conjugate.

Under the condition of larger detuning, i.e., $\Delta_{x,yz} \gg g_{x,k}$, Ω_x , the probability that the excited atomic states are populated is virtual, then the Hamiltonian (2) is reduced to an effective one that involves only the Stark shifts induced respectively by the classical and cavity fields for the three ground states, and Raman transitions $|g_0\rangle \rightarrow |g_k\rangle$ ($k = L, R$) induced collectively by the classical and cavity fields (See Appendix A). Furthermore, to avoid excitation of real photonic states in the cavities and fiber, we first set $\mu_1 \equiv \frac{\Omega_A^2}{\Delta_{A,e_0 g_0}} = \frac{\Omega_B^2}{\Delta_{B,e_k g_k}}$, $\mu_2 \equiv \frac{g_{A,k}^2}{\Delta_{A,e_0 g_k}} = \frac{g_{B,k}^2}{\Delta_{B,e_k g_0}}$, $\lambda \equiv \frac{g_{A,k} \Omega_A}{2} (\frac{1}{\Delta_{A,e_0 g_0}} + \frac{1}{\Delta_{A,e_0 g_k}}) = \frac{g_{B,k} \Omega_B}{2} (\frac{1}{\Delta_{B,e_k g_0}} + \frac{1}{\Delta_{B,e_k g_k}})$, $\Delta \equiv \Delta_{A,e_0 g_k} - \Delta_{A,e_0 g_0} = \Delta_{B,e_k g_0} - \Delta_{B,e_k g_k}$, $\phi_A = \phi_B$ and $\nu = \nu_k$, and satisfy the condition $\sqrt{2}\nu$, $|\Delta - \sqrt{2}\nu|$, $\Delta + \sqrt{2}\nu$, and $\Delta \gg \frac{\mu_2}{4}$, $\frac{\lambda}{2}$. In this case, the energy exchange between the atoms and the photonic modes of the cavities and fiber is also virtual (see Appendix A). Suppose all the modes of the cavities and fiber are initially in the vacuum state, i.e., $|00\rangle_{c_1} |00\rangle_{fib} |00\rangle_{c_2}$. Thus all these modes will remain in the vacuum state during the evolution. Therefore, the global effective Hamiltonian reads [29]

$$H_e'' = \sum_{k=L,R} \eta (|g_0\rangle_A \langle g_0| + |g_k\rangle_B \langle g_k|) - \chi (e^{-i\varphi_f} S_{A,k}^\dagger S_{B,k}^- + H.c), \quad (3)$$

where

$$\eta = \mu_1 + \frac{\lambda^2}{4} \left[\left(\frac{1}{\Delta - \sqrt{2}\nu} + \frac{1}{\Delta + \sqrt{2}\nu} + \frac{2}{\Delta} \right), \quad (4)$$

$$\chi = \frac{\lambda^2}{4} \left(-\frac{1}{\Delta - \sqrt{2}\nu} - \frac{1}{\Delta + \sqrt{2}\nu} + \frac{2}{\Delta} \right), \quad (5)$$

$S_{A,k}^\dagger = |g_0\rangle_A \langle g_k|$, and $S_{B,k}^- = |g_0\rangle_B \langle g_k|$. The Hamiltonian (3) allows for the global coherent manipulation of the atomic states. We will show this in detail by studying the generation of qutrit entanglement between the two distant atoms.

3. Generation of qutrit entanglement

We now show that the effective Hamiltonian (3) allows one to generate a qutrit-qutrit entangled state between two atoms A and B . Initially, the two cavities and the fibre are in the vacuum state while the two atoms are initialised in $|\psi_{AB}(0)\rangle \equiv |g_0\rangle_A |g_0\rangle_B$ (this can be achieved by optical pumping with two classical laser fields, one at resonance with the transition from $F = 2$ to $F' = 2$, the other one coupling to the transition from $F = 1$ to $F' = 2$ [30]). From the effective Hamiltonian (3), we immediately obtain the temporal evolution of the two atoms as follows:

$$|\psi_{AB}(t)\rangle = e^{-i\mu t} [\cos(\sqrt{2}\chi t) |g_0\rangle_A |g_0\rangle_B + \frac{i}{\sqrt{2}} e^{-i\varphi_f} \sin(\sqrt{2}\chi t) (|g_L\rangle_A |g_L\rangle_B + |g_R\rangle_A |g_R\rangle_B)]. \quad (6)$$

Setting $\chi t = \frac{\arctan(\sqrt{2}) + m\pi}{\sqrt{2}}$ ($m = 0, 1, 2, \dots$), we get a qutrit-qutrit maximally entangled state (in the sense that the local Von Neumann entropy is maximal)

$$|\psi_{AB}^{3D}\rangle = \frac{e^{-i\mu t}}{\sqrt{3}} [|g_0\rangle_A |g_0\rangle_B + ie^{-i\varphi_f} (|g_L\rangle_A |g_L\rangle_B + |g_R\rangle_A |g_R\rangle_B)]. \quad (7)$$

The scheme is deterministic and viable for a rather wide range of system parameters. It should be noted that the process for the generation of the qutrit-qutrit entangled state in the present scheme is at variance with previous strategies adopting dispersive interactions [27], because here the occupation of both the atomic excited states *and* of the photonic states in the cavities and fibre are negligible. Moreover, the external control in the present scheme is less demanding, as the preparatory step to put the atom in a specific superposition of two ground states [25,27] or the local manipulation of one of the atoms (by yet another classical field) during the temporal evolution of the whole system [25], are not required here.

In the above analysis, exact knowledge of the system parameters is assumed. But, in general, there could be various errors in the parameters due to the imperfect characterisation of the system. The potential errors include:

- the mismatch of the coupling rate $g_{x,k}$ and Ω_x ($x = A, B$; $k = L, R$.) for the atoms with the local cavity and classical fields, as $g_{x,k}$ and Ω_x are dependent on the atomic position and might fluctuate;
- the mismatch of the phase ϕ_x due to noise in the phases of the classical fields;
- the mismatch of the detuning $\Delta_{x,yz}$ ($x = A, B$; $y = e_0, e_L, e_R$; and $z = g_0, g_L, g_R$) between atoms and fields due to possibly imprecise control;
- the mismatch of the coupling rate ν_k for the cavity and fibre modes, as ν_k is decided by the manufacture technology and might be imprecise;
- timing errors, due to the finite switching rates of the interactions and the limited precisions of the interaction times (t_A and t_B will be set for each atom interacting with the local fields.);
- polarisation errors due to unstable magnetic fields, which lead to mismatches in two parameters related to polarisation, such as $g_{x,L(R)}$, $\nu_{L(R)}$ and $\Delta_{x,L(R)}$ ($\Delta_{x,L(R)}$ here denotes the detuning for $\pi - \sigma^+$ or $\pi - \sigma^-$ Raman channel).

In order to check out how the mentioned errors influence the generation of the entangled state, we define the following fidelity as a measure of the reliability of the qutrit-qutrit maximally entangled state:

$$F = \langle \psi_{AB}^{3D} | Tr_{c_1, f, c_2} [\rho(t)] | \psi_{AB}^{3D} \rangle, \quad (8)$$

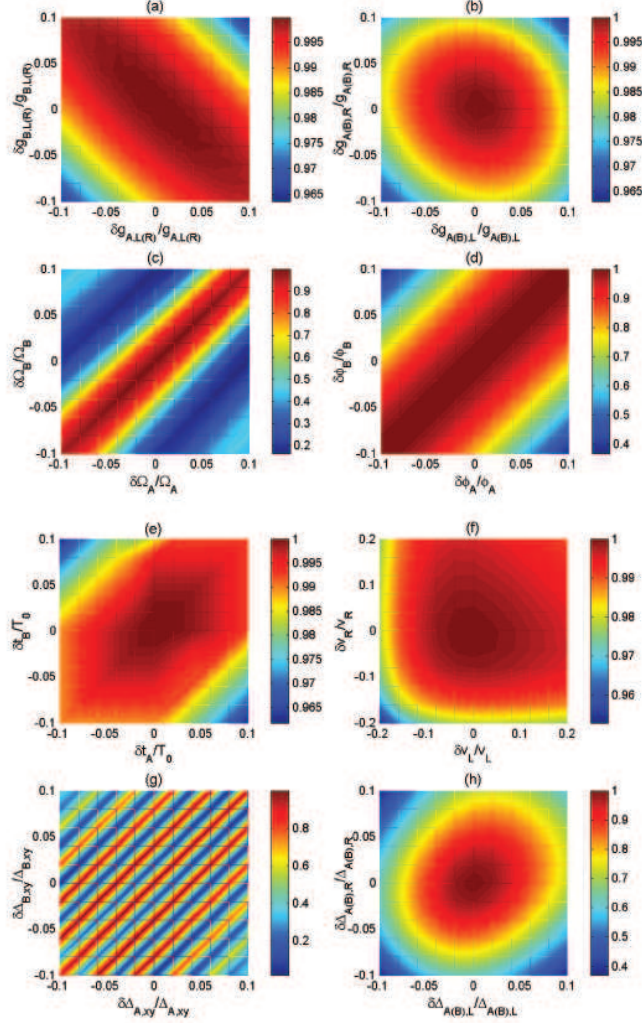


Figure 2. The fidelity of the qutrit-qutrit entangled state versus kinds of errors (all the parameters plotted are dimensionless). (a) F vs $\frac{\delta g_{A,L(R)}}{g_{A,L(R)}}$ and $\frac{\delta g_{B,L(R)}}{g_{B,L(R)}}$; (b) F vs $\frac{\delta g_{A(B),L}}{g_{A(B),L}}$ and $\frac{\delta g_{A(B),R}}{g_{A(B),R}}$; (c) F vs $\frac{\delta \Omega_A}{\Omega_A}$ and $\frac{\delta \Omega_B}{\Omega_B}$; (d) F vs $\frac{\delta \phi_A}{\phi_A}$ and $\frac{\delta \phi_B}{\phi_B}$; (e) F vs $\frac{\delta t_A}{T_0}$ and $\frac{\delta t_B}{T_0}$; (f) F vs $\frac{\delta v_L}{v_L}$ and $\frac{\delta v_R}{v_R}$; (g) F vs $\frac{\delta \Delta_{A,xy}}{\Delta_{A,xy}}$ and $\frac{\delta \Delta_{B,xy}}{\Delta_{B,xy}}$; and (h) F vs $\frac{\delta \Delta_{A(B),L}}{\Delta_{A(B),L}}$ and $\frac{\delta \Delta_{A(B),R}}{\Delta_{A(B),R}}$.

where $\rho(t)$ is the state of the entire system at arbitrary time (governed by Eq. (9), where neither decoherence nor errors are accounted for), and $Tr_{c1,f,c2}$ denotes the partial trace over the field degrees of freedom.

We first assume “perfect” interactions, considering the case $g_{x,k} \equiv g$, $\Omega_x = \Omega \equiv g$, $\Delta_{A,e_0g_0} = \Delta_{B,e_kg_k} \equiv 20g$, $\Delta_{A,e_0g_k} = \Delta_{B,e_kg_0} \equiv 21g$, $\phi_A \equiv \phi_B$, and $\nu_k = v \equiv \sqrt{2}g$) as a reference. Under such conditions maximal qutrit-qutrit entanglement is obtained at the reference time $t = T_0$ (in the notation of the previous section, only the case

$m = 0$ is considered, *i.e.*, $\chi T_0 \equiv 0.6755$). We then set the errors involved in the parameters $g_{x,k}$, Ω_x , $\Delta_{x,yz}$, ν_k , ϕ_k and t_x to be $\delta g_{x,k}$, $\delta \Omega_x$, $\delta \Delta_{x,yz}$, $\delta \nu_k$, $\delta \phi_k$ and δt_x , respectively. In Fig. 2, the fidelity is plotted versus the different kinds of errors. Notice that these fidelity plots display a number of symmetries. The mirror symmetries about the line bisecting the axes trivially reflect the choices of the error parameters and the symmetry of the system under exchange of the two atoms and cavities. Some of the symmetries are instead more interesting: for instance, errors in the detunings induce additional phases and have clearly oscillatory effects (g), errors in the cavity-fibre coupling strengths induce different Stark shifts (and have hence different effects) depending on their signs (f), while errors in the atom-light coupling strengths in the two different polarisations have, more intriguingly, approximately ‘rotationally symmetric’ effects (b). Let us now quantitatively discuss the influence of the various kinds of errors on the fidelity with the entangled ‘reference state’.

It can be seen from Fig. 2 (a), (b), (e) and (f) that the fidelity F is very robust against errors in the parameters $g_{x,k}$, ν_k and t_x . A deviation $|\delta g_{x,k}| \simeq 10\% g_{x,k}$, $|\delta \nu_x| \simeq 10\% \nu_x$, or $|\delta t_x| \simeq 10\% T_0$ will cause only a reduction smaller than 10^{-2} in the fidelity.

From Fig. 2 (c), it is apparent that the fidelity is, on the other hand, very sensitive to imperfections in Ω_x , mainly dependent on the Stark shifts induced by the classical fields [see Eq. (3)]. However, the influences of imperfect Ω_x through such Stark shifts can be eliminated as one can apply a second classical field to produce offsetting ac-Stark shifts on both atoms [27]. If this is done, then the effect of the errors $|\delta \Omega_x|$ on Ω_x will be analogous to the effect of the deviation $|\delta g_{x,k}|$ in $g_{x,k}$, which have already been shown to be very slight. Thus, this simple countermeasure would make the entanglement fidelity robust also against possible errors in Ω_x .

When deriving the effective Hamiltonian (3), we set the condition $\phi_A \equiv \phi_B$ to eliminate the phases of the classical fields in Eq. (3) (see Appendix A). However, such phases are affected by noise and fluctuations, and might be slightly different in practical instances. Nevertheless, the fidelity is only marginally degraded by the possible errors in the parameter ϕ_x : a deviation $|\delta \phi_k| = 3\% \phi_k$ will cause only 2% in the reduction of the fidelity. In practice, Using only one classical field to illuminate both atoms that are distributed in the two cavities would help in keeping the phase fluctuations under control [31].

Let us remind the reader that in our scheme the cavity and the classical fields are detuned from the corresponding atomic transitions by specific values. It can be seen from Fig. 2 (g) that the fidelity is highly dependent on the parameter $\Delta_{x,yz}$: a small deviation in $\Delta_{x,yz}$ leads to large oscillation in the fidelity. This is mainly due to the detuning-dependent Stark shifts induced by the cavity and classical fields, besides the possible occurrence of a phase ($\Delta = \Delta_{A,e_0 g_k} - \Delta_{A,e_0 g_0} - \Delta_{B,e_k g_0} + \Delta_{B,e_k g_k}$) in the exponential factor $e^{i\Delta t}$ in Eq. (3). Though this requirement is strict, it is not a major problem with the currently developed laser technology in cavity QED experiments: the necessary stabilisation of the fields’ frequencies can be achieved by means of acousto-optic modulators [32]. In Fig. 2 (h), we check the stability of the fidelity versus the detunings for the two polarisation ($\pi - \sigma^+$ or $\pi - \sigma^-$) Raman channels. Ideally, the conditions $\Delta_{A,L} = \Delta_{A,R}$ and $\Delta_{B,L} = \Delta_{B,R}$ are required. But, in real experiments, this requirement may not be perfectly satisfied, due to the fact that the magnetic field can break the degeneracy between the atomic ground states. Our investigation, reported in Fig. 2 (h) shows that the fidelity is only slightly affected by errors in the detunings for both polarisation channels: the fidelity with the entangled state of reference will

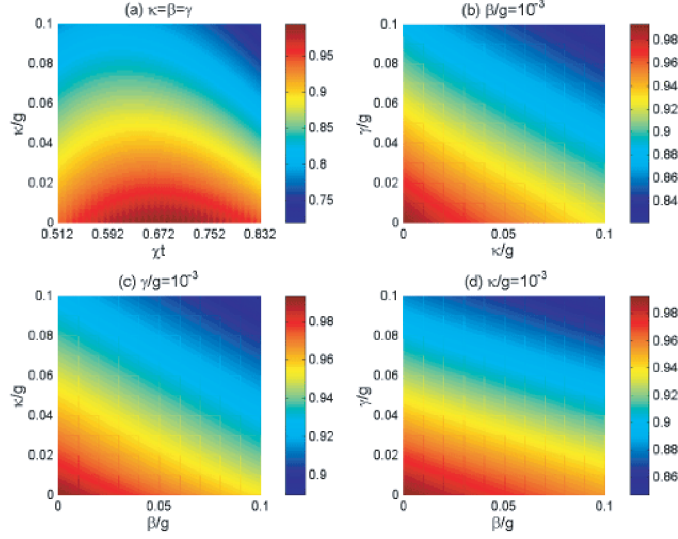


Figure 3. The fidelity of the qutrit-qutrit entangled state versus the dimensionless parameters χt , κ/g , γ/g or β/g . (a) F vs χt and κ/g ($\kappa = \beta = \gamma$); (b) F vs κ/g and γ/g ($\beta = 10^{-3}g$); (c) F vs γ/g and β/g ($\kappa = 10^{-3}g$); and (d) F vs κ/g and β/g ($\gamma/g = 10^{-3}g$).

still be larger than 0.96 even when a deviation $|\delta\Delta_{A(B),k}| \simeq 3\%\Delta_{A(B),k}$ occurs.

4. Influence of spontaneous emission and photon leakage

In all the above arguments, we have assumed the entire system is ideally isolated from the environment, and have not considered any dissipation. In this section, we take into account the dissipation due to atomic spontaneous emission and photon leakage from the cavities and fibre. The master equation for the density matrix of the entire system can be expressed as

$$\begin{aligned} \dot{\rho} = & -i[H_{full}, \rho] + \frac{\kappa}{2} \sum_{k=L,R} \left[\sum_{x=A,B} (2a_{x,k}\rho a_{x,k}^\dagger - a_{x,k}^\dagger a_{x,k}\rho - \rho a_{x,k}^\dagger a_{x,k}) \right. \\ & + \frac{\beta}{2} (2b_k\rho b_k^\dagger - b_k^\dagger b_k\rho - \rho b_k^\dagger b_k) \Big] \\ & + \frac{\gamma}{2} \sum_{x=A,B} \sum_{\sigma=L,R,\pi} (2A_{x,\sigma}\rho A_{x,\sigma}^\dagger - A_{x,\sigma}^\dagger A_{x,\sigma}\rho - \rho A_{x,\sigma}^\dagger A_{x,\sigma}), \end{aligned} \quad (9)$$

where $A_{x,\sigma} = \sum_{y,z} |y\rangle_x \langle y; 1\sigma | z\rangle_x \langle z|$ ($y = g_L, g_0, g_R$; $z = e_L, e_0, e_R$) is the atomic lowering operator, with ${}_x \langle y; 1\sigma | z\rangle_x$ being the Clebsch-Gordan coefficient (i.e., $C_{m,m'}$) for the dipole transition $|e\rangle \leftrightarrow |g\rangle$ with polarisation $\sigma = L, R, \pi$; γ , β and κ stand, respectively, for the spontaneous emission rate and for the fibre and cavity decay rates (assumed for simplicity to be equal for the two cavities and for the two polarised modes). The contribution of the thermal photons have been neglected, as is possible at optical frequencies.

The master equation (9) has been numerically solved in the subspace $\Gamma \in \{\Gamma_{full}, |g_L\rangle_A |g_0\rangle_B |00\rangle_{c_1} |00\rangle_{fib} |00\rangle_{c_2}, |g_R\rangle_A |g_0\rangle_B |00\rangle_{c_1} |00\rangle_{fib} |00\rangle_{c_2}\}$. In Fig. 3 (a), the

fidelity of the maximal qutrit-qutrit entangled state is plotted versus the dimensionless parameters χt and κ/g ($\kappa = \beta = \gamma$ is set). In Fig. 3 (b), (c) and (d) the fidelity is plotted versus each pair of the three dimensionless parameters κ/g , β/g and γ/g (the remaining one is set to be $10^{-3}g$). In the calculations, we still set $\Omega_A = \Omega_B = g_{A,k} = g_{B,k} \equiv g$, $\Delta_{A,e_0g_0} = \Delta_{B,e_kg_k} \equiv 20g$, $\Delta_{A,e_0g_k} = \Delta_{B,e_kg_0} \equiv 21g$, and $\nu_k \equiv \sqrt{2}g$.

From Fig. 3 (a), we note that the fidelity is almost unaffected by the three decay rates κ , β and γ when $\kappa = \beta = \gamma = 10^{-3}g$. Even when $\kappa = \beta = \gamma = 10^{-2}g$, the fidelity is close to 0.97, which is much larger than the one (< 0.87) obtained in Ref. [27]. This improvement is of course due to the suppression of the excited states' population of the fields, as well as of the atoms. From Fig. 3 (b), (c) and (d), it can be seen that a decay rate of $10^{-2}g$, for either κ , β or γ alone (with the other two parameters set to zero) leads to a fidelity larger than 0.98. Note that the previous scheme through the adiabatic passage [25], a decay rate $\kappa \equiv 10^{-2}g$ alone degraded the fidelity down to $F = 0.95$.

5. Conclusion

In summary, we have proposed a scheme of atomic levels (with an explicit possible realisation in Zeeman sublevels of alkali atoms), where qutrit quantum information can be stored in three ground states and, most importantly, manipulated globally between distant nodes through the virtual excitation of excited atomic levels and mediating bosonic fields like, typically, light.

Our scheme is different from any previously proposed ones in that this choice of atomic levels allows for the whole coherent evolution of the global system – involving the two atoms and the linking bosonic modes – to be driven by the virtual excitation of *both* the atomic excited levels *and* the intervening fields.

This feature renders our scheme remarkably more robust than any other previously proposed in the face of decoherence, whose main sources in these settings are photon loss and spontaneous emission from excited levels. Also, our scheme – being based, essentially, on the proper choice of atomic levels and operating regimes – requires very modest control and proves to be rather resilient against experimental imperfections as well. All these qualitative remarks have been substantiated in this work by a very thorough quantitative analysis of such unwanted effects.

Clearly, a price has to be paid for improved robustness: the use of exclusively virtual excitations makes these coherent manipulations very slow if compared to schemes adopting resonant couplings [33]. Ultimately, the choice between faster, resonant schemes and more robust, virtual ones should depend on the use one intends to make of them. Of course, speed would be paramount in applications directly related to quantum computation. However, as pointed out in the introduction, qutrit systems are mainly interesting for quantum communication purposes, where the most delicate task to accomplish is precisely the robust distribution of entanglement between distant nodes of a network, and speed is not as crucial: the present, fully virtual scheme would respond precisely to this need. In this perspective, our study shows that atomic systems hold considerable promise for the encoding and coherent, distributed manipulation of multidimensional quantum alphabet for quantum communication purposes.

Appendix A: Derivation of the effective Hamiltonian

Under the condition of large detuning, *i.e.* for $\Delta_{x,yz} \gg g_{x,k}$, Ω_x , and as long as the atoms are initialised in the ground states, the probability that the atomic excited states are populated is virtual. Thus, the atomic excited states are negligible during the time evolution of the entire system. In this case, we can adopt the time-averaging method [34] to obtain an effective Hamiltonian as follows [35]:

$$\begin{aligned}
H_e^{acl} &= -iH_I^{acl}(t) \int H_I^{acl}(t') dt' \\
&= \sum_{k=L,R} [\mu_{\Omega_A} |g_0\rangle_A \langle g_0| + \mu_{\Omega_B} |g_k\rangle_B \langle g_k| \\
&\quad + \mu_{a_{A,k}} a_{A,k}^\dagger a_{A,k} |g_k\rangle_A \langle g_k| + \mu_{a_{B,k}} a_{B,k}^\dagger a_{B,k} |g_0\rangle_B \langle g_0| \\
&\quad + \lambda_{a_{A,k}\Omega_A} (a_{A,k} e^{i\Delta_{A,k}t} e^{-i\phi_A} |g_0\rangle_A \langle g_k| + H.c) \\
&\quad + \lambda_{a_{B,k}\Omega_B} (a_{B,k} e^{i\Delta_{B,k}t} e^{-i\phi_B} |g_k\rangle_B \langle g_0| + H.c)], \tag{10}
\end{aligned}$$

where $\mu_{\Omega_A} = \frac{\Omega_A^2}{\Delta_{A,e_0g_0}}$, $\mu_{\Omega_B} = \frac{\Omega_B^2}{\Delta_{B,e_kg_k}}$, $\mu_{a_{A,k}} = \frac{g_{A,k}^2}{\Delta_{A,e_0g_k}}$, $\mu_{a_{B,k}} = \frac{g_{B,k}^2}{\Delta_{B,e_kg_0}}$, $\lambda_{a_{A,k}\Omega_A} = \frac{g_{A,k}\Omega_A}{2}(\frac{1}{\Delta_{A,e_0g_0}} + \frac{1}{\Delta_{A,e_0g_k}})$, $\lambda_{a_{B,k}\Omega_B} = \frac{g_{B,k}\Omega_B}{2}(\frac{1}{\Delta_{B,e_kg_0}} + \frac{1}{\Delta_{B,e_kg_k}})$, $\Delta_{A,k} = \Delta_{A,e_0g_k} - \Delta_{A,e_0g_0}$, $\Delta_{B,k} = \Delta_{B,e_kg_0} - \Delta_{B,e_kg_k}$. For H_e^{acl} in Eq. (10), the first (second) and third (fourth) terms describe the Stark shifts for the states $|g_0\rangle$ ($|g_k\rangle$) and $|g_k\rangle$ ($|g_0\rangle$) of the atom in cavity A (B), induced by the classical and cavity fields, respectively; the fifth (sixth) term describes the Raman coupling between the states $|g_0\rangle$ and $|g_k\rangle$ for the atom in cavity A (B), induced collectively by the classical and cavity fields.

Hence, the effective Hamiltonian of the entire system is given by $H_e = H_I^{cf} + H_e^{acl}$. Let us now introduce three normal modes c_k and $c_{\pm k}$ by applying the canonical transformation $c_k = \frac{1}{\sqrt{2}}(a_{A,k} - e^{-i\varphi_f} a_{B,k})$ and $c_{\pm k} = \frac{1}{2}(a_{A,k} + e^{-i\varphi_f} a_{B,k} \pm \sqrt{2}b_k)$ [22]. Then, we switch to a rotating frame by the unitary transformation $R = e^{-iH_I^{cf}t}$ [29], *i.e.*, $H'_e = R^\dagger H_e R - iR^\dagger \frac{dR}{dt}$, and obtain

$$\begin{aligned}
H'_e &= \sum_{k=L,R} \{ \mu_{\Omega_A} |g_0\rangle_A \langle g_0| + \mu_{\Omega_B} |g_k\rangle_B \langle g_k| \\
&\quad + \frac{\mu_{a_{A,k}}}{4} (c_{+k}^\dagger c_{+k} + c_{-k}^\dagger c_{-k} + 2c_k^\dagger c_k) |g_k\rangle_A \langle g_k| \\
&\quad + \frac{\mu_{a_{B,k}}}{4} (c_{+k}^\dagger c_{+k} + c_{-k}^\dagger c_{-k} + 2c_k^\dagger c_k) |g_0\rangle_B \langle g_0| \\
&\quad + \frac{\mu_{a_{A,k}}}{4} (c_{+k}^\dagger c_{-k} e^{i2\sqrt{2}\nu_k t} + \sqrt{2}c_{+k}^\dagger c_k e^{i\sqrt{2}\nu_k t} + \sqrt{2}c_{-k}^\dagger c_k e^{-i\sqrt{2}\nu_k t} + H.c) |g_k\rangle_A \langle g_k| \\
&\quad + \frac{\mu_{a_{B,k}}}{4} (c_{+k}^\dagger c_{-k} e^{i2\sqrt{2}\nu_k t} - \sqrt{2}c_{+k}^\dagger c_k e^{i\sqrt{2}\nu_k t} - \sqrt{2}c_{-k}^\dagger c_k e^{-i\sqrt{2}\nu_k t} + H.c) |g_0\rangle_B \langle g_0| \\
&\quad + \frac{\lambda_{a_{A,k}\Omega_A}}{2} [(c_{+k} e^{-i\sqrt{2}\nu_k t} + c_{-k} e^{i\sqrt{2}\nu_k t} + \sqrt{2}c_k) e^{i\Delta_{A,k}t} e^{-i\phi_A} |g_0\rangle_A \langle g_k| + H.c] \\
&\quad + \frac{\lambda_{a_{B,k}\Omega_B}}{2} [(c_{+k} e^{-i\sqrt{2}\nu_k t} + c_{-k} e^{i\sqrt{2}\nu_k t} - \sqrt{2}c_k) e^{i\Delta_{B,k}t} e^{-i(\phi_B - \varphi_f)} |g_k\rangle_B \langle g_0| + H.c] \}.
\end{aligned}$$

For simplicity, we now set $\mu_1 = \mu_{\Omega_A} = \mu_{\Omega_B}$, $\mu_2 = \mu_{a_{A,k}} = \mu_{a_{B,k}}$, $\lambda = \lambda_{a_{A,k}\Omega_A} = \lambda_{a_{B,k}\Omega_B}$, $\Delta = \Delta_{A,k} = \Delta_{B,k}$, $\phi_A = \phi_B$ and $\nu = \nu_k$. Under the condition $\sqrt{2}\nu$,

$|\Delta - \sqrt{2}\nu|$, $\Delta + \sqrt{2}\nu$, and $\Delta \gg \frac{\mu_2}{4}$, $\frac{\lambda}{2}$, the energy exchange between the bosonic modes and the atoms as well as between the bosonic modes themselves is virtual. The virtual excitation of the bosonic modes leads to the Stark shifts and coupling between the atoms. Then H'_e reduces to [29]

$$\begin{aligned}
H''_e = & \sum_{k=L,R} \{ \mu_1 (|g_0\rangle_A \langle g_0| + |g_k\rangle_B \langle g_k|) \\
& + \frac{\mu_2}{4} (c_{+k}^\dagger c_{+k} + c_{-k}^\dagger c_{-k} + 2c_k^\dagger c_k) (|g_k\rangle_A \langle g_k| + |g_0\rangle_B \langle g_0|) \\
& + \frac{\mu_2^2}{32\sqrt{2}\nu} (c_{+k}^\dagger c_{+k} - c_{-k}^\dagger c_{-k}) (|g_k\rangle_A \langle g_k| + |g_0\rangle_B \langle g_0|)^2 \\
& + \frac{\mu_2^2}{8\sqrt{2}\nu} (c_{+k}^\dagger c_{+k} - c_{-k}^\dagger c_{-k}) (|g_k\rangle_A \langle g_k| - |g_0\rangle_B \langle g_0|)^2 \\
& + \frac{\lambda^2}{4} [(\frac{1}{\Delta - \sqrt{2}\nu} c_{+k} c_{+k}^\dagger + \frac{1}{\Delta + \sqrt{2}\nu} c_{-k} c_{-k}^\dagger + \frac{2}{\Delta} c_k c_k^\dagger) (|g_0\rangle_A \langle g_0| + |g_k\rangle_B \langle g_k|) \\
& - (\frac{1}{\Delta - \sqrt{2}\nu} c_{+k}^\dagger c_{+k} + \frac{1}{\Delta + \sqrt{2}\nu} c_{-k}^\dagger c_{-k} + \frac{2}{\Delta} c_k^\dagger c_k) (|g_k\rangle_A \langle g_k| + |g_0\rangle_B \langle g_0|)] \\
& - \frac{\lambda^2}{4} (-\frac{1}{\Delta - \sqrt{2}\nu} - \frac{1}{\Delta + \sqrt{2}\nu} + \frac{2}{\Delta}) (e^{-i\varphi_f} S_{A,k}^\dagger S_{B,k}^- + H.c.) \}, \tag{11}
\end{aligned}$$

with $S_{A,k}^\dagger = |g_0\rangle_A \langle g_k|$ and $S_{B,k}^- = |g_0\rangle_B \langle g_k|$. The quantum-number operators $c_{+k}^\dagger c_{+k}$, $c_{-k}^\dagger c_{-k}$, $c_k^\dagger c_k$ for the bosonic modes are conserved quantities during the interaction as all of them commute with the Hamiltonian H''_e . Suppose all the modes of the cavities and fibre are initially in the vacuum state, i.e., $|00\rangle_{c_1} |00\rangle_{fib} |00\rangle_{c_2}$. Hence, all the bosonic modes c_{+k} , c_{-k} and c_k will remain in the vacuum state during the evolution.

Finally, the global effective Hamiltonian H''_e reads

$$H''_e = \sum_{k=L,R} \eta (|g_0\rangle_A \langle g_0| + |g_k\rangle_B \langle g_k|) - \chi (e^{-i\varphi_f} S_{A,k}^\dagger S_{B,k}^- + H.c.), \tag{12}$$

where

$$\eta = \mu_1 + \eta', \tag{13}$$

$$\eta' = \frac{\lambda^2}{4} [(\frac{1}{\Delta - \sqrt{2}\nu} + \frac{1}{\Delta + \sqrt{2}\nu} + \frac{2}{\Delta})], \tag{14}$$

and

$$\chi = \frac{\lambda^2}{4} (-\frac{1}{\Delta - \sqrt{2}\nu} - \frac{1}{\Delta + \sqrt{2}\nu} + \frac{2}{\Delta}). \tag{15}$$

It should be noted that we have neglected the term $\eta' |g_0\rangle_A \langle g_0|$ to maintain the symmetry in the effective Hamiltonian (12). In practice, this term can be compensated by an additional ac-Stark shift for the state $|g_0\rangle$ of atom A [27].

Appendix B: Validity of the effective dynamics

We now turn back to the full Hamiltonian of the system and check how accurate is the description of the system through the effective Hamiltonian (3). We take the energy

level $|F = 2\rangle$ of $5^2S_{1/2}$ to be the zero energy reference point, and write down the full Hamiltonian for the entire system as follows:

$$\begin{aligned}
H_{full} = & \sum_{k=L,R} (\omega_{f,k} b_k^\dagger b_k + \omega_{a_{A,k}} a_{A,k}^\dagger a_{A,k} + \omega_{a_{B,k}} a_{B,k}^\dagger a_{B,k} \\
& \omega_{A,g_k} |g_k\rangle_A \langle g_k| + \omega_{B,e_k} |e_k\rangle_B \langle e_k|) + \omega_{A,e_0} |e_0\rangle_A \langle e_0| + \omega_{B,g_0} |g_0\rangle_B \langle g_0| \\
& + \sum_{k=L,R} [g_{A,k} a_{A,k} |e_0\rangle_A \langle g_k| + \Omega_A e^{-i(\omega_{\Omega_A} t - \phi_A)} |e_0\rangle_A \langle g_0| \\
& + g_{B,k} a_{B,k} |e_k\rangle_B \langle g_0| + \Omega_B e^{-i(\omega_{\Omega_B} t - \phi_B)} |e_k\rangle_B \langle g_k| + H.c] \\
& + \sum_{k=L,R} \nu_k [b_k (a_{A,k}^\dagger + e^{i\varphi_f} a_{B,k}^\dagger) + H.c], \tag{16}
\end{aligned}$$

where $\omega_{f,k}$ and $\omega_{a_{A,k}}$ ($\omega_{a_{B,k}}$) are the energy levels for the polarised photons in the fibre and cavity A (B), respectively, ω_{Ω_x} ($x = A, B$) denotes the energy for the π -polarised classical field Ω_x , and $\omega_{x,m}$ ($m = g_0, g_k, e_0, e_k$) is the energy level for the atomic state $|m\rangle_x$.

Taking the initial state $|\psi(0)\rangle = |g_0\rangle_A |g_0\rangle_B |00\rangle_{c_1} |00\rangle_{fib} |00\rangle_{c_2}$ and considering all possible states of the system in evolution, we express the state of the system at time t as $|\psi_{full}(t)\rangle = \sum_i c_i(t) |\phi_i\rangle$ ($c_i(t)$ being time-dependent amplitudes) within the subspace Γ_{full} spanned by the vectors $\{|\phi_1\rangle, \dots, |\phi_i\rangle, \dots, |\phi_{12}\rangle\}$:

$$\begin{aligned}
\Gamma_{full} \equiv & \{(|g_0\rangle_A |g_0\rangle_B, |e_0\rangle_A |g_0\rangle_B, |g_L\rangle_A |g_L\rangle_B, |g_R\rangle_A |g_R\rangle_B, |g_L\rangle_A |e_L\rangle_B, |g_R\rangle_A |e_R\rangle_B) \\
& \otimes |00\rangle_{c_1} |00\rangle_{fib} |00\rangle_{c_2}, |g_L\rangle_A |g_0\rangle_B \\
& \otimes (|10\rangle_{c_1} |00\rangle_{fib} |00\rangle_{c_2}, |00\rangle_{c_1} |10\rangle_{fib} |00\rangle_{c_2}, |00\rangle_{c_1} |00\rangle_{fib} |10\rangle_{c_2}), |g_R\rangle_A |g_0\rangle_B \\
& \otimes (|01\rangle_{c_1} |00\rangle_{fib} |00\rangle_{c_2}, |00\rangle_{c_1} |01\rangle_{fib} |00\rangle_{c_2}, |00\rangle_{c_1} |00\rangle_{fib} |01\rangle_{c_2})\}.
\end{aligned}$$

The occupation probability for each state vector $|\phi_i\rangle$ during the evolution is $P_i(t) = |c_i(t)|^2$, and satisfies $\sum_{i=1}^{12} P_i(t) = 1$. Thus the occupation probability of the atomic excited states and the photonic states are $P_e(t) = \sum_{i=2,5,6} P_i$ and $P_p(t) = \sum_{i=7}^{12} P_i$, respectively. The validity of the effective Hamiltonian implies that both the occupation probability $P_e(t)$ and $P_p(t)$ should be small enough thus they can be negligible during the time evolution of the entire system. We focus here on quantum state transfer, *i.e.*, on the variation of the occupation probability $P_1(t)$ and $P_{tra}(t) \equiv \sum_{i=3,4} P_i$, for the numerical verification of the effective dynamics, which is portrayed in Fig. 4. Fig. 4 (a1) and (a2) are obtained through the solution of the Schrödinger equation $i \frac{d|\psi_{eff}(t)\rangle}{dt} = H_e'' |\psi_{eff}(t)\rangle$ in the subspace $\Gamma_e \in \{|\phi_1\rangle, |\phi_3\rangle, |\phi_4\rangle\}$. The two figures display perfect Rabi oscillations, which indicates ideal state transfer between the states $|\phi_1\rangle$ and $1/\sqrt{2}(|\phi_3\rangle + |\phi_4\rangle)$.

Fig. 4 (b1), (c1), (d1), (b2), (c2) and (d2) are obtained through the solution of the Schrödinger equation $i \frac{d|\psi_{full}(t)\rangle}{dt} = H_{full} |\psi_{full}(t)\rangle$ in the subspace Γ_{full} . It can be seen from Fig. 4 (b1) and (b2) that state transfer via the effective Hamiltonian (3) is almost perfect (for Fig. 4 (b2), this is especially apparent.), indicating that numerical results obtained from the effective and full Hamiltonians would be equivalent. Fig. 4 (c1) and (c2) plot the variation of the occupation probability of the atomic excited states, while Fig. 4 (d1) and (d2) plot the variation of the occupation probability of the photonic states in the cavities and fibre. It is apparent that both P_e and P_p are very small during the evolution of the entire system. The analysis above verifies the validity of the effective Hamiltonian (3).

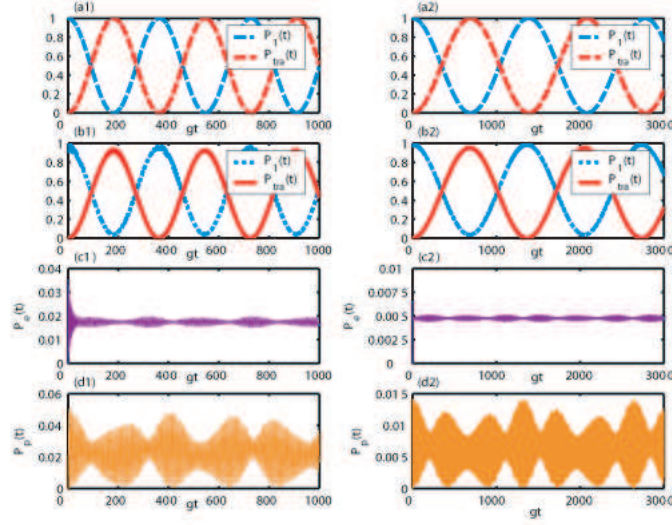


Figure 4. The occupation probability $P_1(t)$, $P_{tra}(t)$, $P_e(t)$ and $P_p(t)$ versus the dimensionless parameter gt , respectively, $\Omega_A = \Omega_B = g_{A,k} = g_{B,k} \equiv g$, $\Delta_{A,e_0g_0} = \Delta_{B,e_kg_k} = \Delta_1$, $\Delta_{A,e_0g_k} = \Delta_{B,e_kg_0} = \Delta_2$ and $\nu \equiv \sqrt{2}g$. (a1) \sim (d1) $\Delta_1 \equiv 10g$, $\Delta_2 \equiv 11g$; (a2) \sim (d2) $\Delta_1 = 20g$, $\Delta_2 = 21g$.

Let us now review the physical conditions given in the description of our system, to reveal some insight about and relationships between certain dynamical parameters when the effective Hamiltonian (3) is valid. In order for H_e'' to hold, we required $\Delta_i \gg g$, Ω as well as $\sqrt{2}\nu$, $|\Delta \pm \sqrt{2}\nu|$, $\Delta \gg \frac{g^2}{4\Delta_i}$, $\frac{g\Omega}{2\Delta_i}$ ($\Delta \ll \Delta_i$, $i = 1, 2$). Δ_i is the dominant factor, because the occupation probability of the atomic excited states (P_e) and the photonic states (P_p) are inversely proportional to Δ_i^2 , given all other parameters are pre-set. This is proved to be true in Fig. 4 (c1), (d1), (c2), and (d2), as the average occupation probability P_e and P_p shown in Fig. 4 (c1) and (d1) are about four times that in Fig. 4 (c2) and (d2). In other words, the difference between the effective Hamiltonian (3) and the full Hamiltonian (16) decreases with increasing Δ_i . This can also explain the phenomena for the different deviation from the perfect state transfer, which are more noticeable in Fig. 4 (b1) than in Fig. 4 (b2).

Let us stress once again that the obtained effective Hamiltonian (3) is indeed valid as the occupations of the atomic excited states and the photonic states have been showed to be strongly suppressed.

Acknowledgments

This work is supported by National Natural Science Foundation of China under Grant No. 10674025 and No. 10974028, the Fujian Natural Science Foundation of China under Grant No. 2009J06002, Doctoral Foundation of the Ministry of Education of China under Grant No. 20070386002, funds from State Key Laboratory Breeding Base of Photocatalysis, Fuzhou University, and funds from Education Department of Fujian Province of China under Grant No. JB08010. SY is supported by a KC Wong Scholarship. AS thanks the Central Research Fund of the University of London for

financial support.

References

- [1] Einstein A, Podolsky B and Rosen N 1935 Phys. Rev. 47 777
- [2] Bell J S 1965 Physics (Long Island City, N.Y.) 1 195
- [3] Greenberger D M, Horne M, Shimony A and Zeilinger A 1990 Am. J. Phys. 58 1131
- [4] Nielsen M A and Chuang I L 2000 *Quantum Computation and Quantum Information* (Cambridge University Press, Cambridge)
- [5] Dür W, Vidal G and Cirac J I 2000 Phys. Rev. A 62 062314
- [6] Kaszlikowski D, Gnacinski P, Zukowski M, Miklaszewski W, Zeilinger A 2000 Phys. Rev. Lett. 85 4418; Collins D, Gisin N, Linden N, Massar S, Popescu S 2002 Phys. Rev. Lett. 88 040404
- [7] Bechmann-Pasquinucci H and Tittel W 2000 Phys. Rev. A 61 062308 Bourennane M, Karlsson A and Bjork G 2001 *ibid.* 64 012306; Walborn S P, Lemelle D S, Almeida M P and Souto Ribeiro P H 2006 Phys. Rev. Lett. 96 090501
- [8] Cirac J I and Zoller P 1995 Phys. Rev. Lett. 74 4091; Monroe C, Meekhof D M, King B E, Itano W M and Wineland D J 1995 *ibid.* 75, 4714; Kielpinski D, Monroe C and Wineland D J, Nature (London) 417 709
- [9] *Cavity Quantum Electrodynamics* 1994 edited by Berman P (Academic, New York); Haroche S and Raimond J M 2006 *Exploring the Quantum* (Oxford University Press, Oxford)
- [10] Esteve D, *Superconducting Qubits*, in Proceedings of the Les Houches 2003 Summer School on Quantum Entanglement and Information Processing 2004 edited by Esteve D and Raimond J M (Elsevier, New York)
- [11] Loss D and DiVincenzo D P 1998 Phys. Rev. A 57 120
- [12] Knill E, Laflamme R and Milburn G J 2001 Nature (London) 409 46; Raussendorf R and Briegel H J 2001 Phys. Rev. Lett. 86 5188
- [13] Kane B 1998 Nature (London) 393 133
- [14] Raimond J M, Brune M and Haroche S 2001 Rev. Mod. Phys. 73 565; Miller R, Northup T E, Birnbaum K M, Boca A, Boozer A D and Kimble H J 2005 J. Phys. B 38 S551; Walther H, Varcoe B T H, Englert B G and Becker T 2006 Rep. Prog. Phys. 69 1325
- [15] Kuhr S et al 2007 Appl. Phys. Lett. 90 164101
- [16] Hagley E, Maitre X, Nogues G, Wunderlich C, Brune M, Raimond J M, Haroche S 1997 Phys. Rev. Lett. 79 1; Osnaghi S, Bertet P, Auffeves, Maioli P, Brune M, Raimond J M, Haroche S Phys. Rev. Lett. 87 037902
- [17] Rauschenbeutel A, Nogues G, Osnaghi S, Bertet P, Brune M, Raimond J M, Haroche S 2000 Science 288 2024
- [18] Zheng S B 2003 Phys. Rev. A 68 035801; Zou X B, Pahlke K and Mathis W 2003 Phys. Rev. A 67 044301
- [19] DiVincenzo D P 2000 Fortschr. Phys. 48 771
- [20] Bose S, Knight P L, Plenio M B and Vedral V 1999 Phys. Rev. Lett. 83 5158; Duan L M and Kimble H J 2003 Phys. Rev. Lett. 90 253601; Feng X L, Zhang Z M, Li X D, Gong S Q and Xu Z Z 2003 Phys. Rev. Lett. 90 217902
- [21] Cirac J I, Zoller P, Kimble H J and Mabuchi H 1997 Phys. Rev. Lett. 78 3221; Pellizzari T, *ibid.* 1997 79 5242
- [22] Serafini A, Mancini S and Bose S 2006 Phys. Rev. Lett. 96 010503
- [23] Kimble H J 2008 Nature (London) 453 1023
- [24] Yin Z Q and Li F L 2007 Phys. Rev. A 75 012324
- [25] Ye S Y, Zhong Z R and Zheng S B 2008 Phys. Rev. A 77 014303
- [26] Zheng S B 2009 Eur. Phys. J. D 54 1434
- [27] Lü X Y, Liu J B, Ding C L and Li J H 2008 Phys. Rev. A 78 032305
- [28] Lü X Y, Si L G, Hao X Y and Yang X 2009 Phys. Rev. A 79 052330
- [29] Zheng S B 2009 Appl. Phys. Lett. 94 154101; Zheng S B 2009 accepted by Chin. Phys. B
- [30] Wilk T, Webster S C, Kuhn A, Rempe G 2007 Science 317 488
- [31] Talab M A, Guérin S, Sangouard N and Jauslin H R 2005 Phys. Rev. A 71 023805
- [32] Hennrich M, Legero T, Kuhn A and Rempe G 2000 Phys. Rev. Lett. 23 4872
- [33] Yang Z B and Zheng S B, in preparation
- [34] James D F V 2000 Fortschr. Phys. 48 823
- [35] Wu Y 1996 Phys. Rev. A 54 1586; Wu Y and Yang X 2005 Phys. Rev. A 71 053806; James D F V and Jerke J 2007 Can. J. Phys. 85 625